Microfiltration Device For Circulating Tumor Cells Isolation (MEMS)-(CTCS)

Dispositivo de microfiltración para el aislamiento de células tumorales circulantes (MEMS)-(CTCS)

Dispositivo de microfiltração para o isolamento de células tumorais circulantes (MEMS)-(CTCS)

Alan Javier González Díaz[1]
Carlos Borrás Pinilla[2]

Received: October 7th, 2022
Accepted: January 15th, 2023
Available: January 22th, 2023

How to cite this article:
A.J. González Díaz, C.B. Borrás Pinilla, "Microfiltration Device For Circulating Tumor Cells Isolation (MEMS)-(CTCS)," *Revista Ingeniería Solidaria,* vol. 19, no. 1, 2023.
doi: https://doi.org/10.16925/2357-6014.2023.01.04

Research article. https://doi.org/10.16925/2357-6014.2023.01.04

[1] Profesional Ingeniero Mecánico, Programa de maestría en ingeniería mecánica, Escuela de ingeniería mecánica, Universidad Industrial de Santander, Bucaramanga, Colombia.

Email: alan2208436@correo.uis.edu.co

ORCID: https://orcid.org/0000-0001-8811-3349

CvLAC: https://scienti.minciencias.gov.co/cvlac/visualizador/generarCurriculoCv.do?cod_rh=0001641712

[2] Doctor en Ingeniería Mecánica, Universidad Industrial de Santander, Bucaramanga, Colombia.

Email: cborras@uis.edu.co

ORCID: https://orcid.org/0000-0002-1014-2817

CvLAC: https://scienti.minciencias.gov.co/cvlac/visualizador/generarCurriculoCv.do?cod_rh=0000716480

Abstract

Introduction: The article is the product of the research "Design and simulation of a microfiltration device for the isolation of circulating tumor cells developed at the Universidad Industrial de Santander in the year 2022

Objective: To design a device to classify and separate circulating tumor cells in blood fluid by using a multi-physics dynamics computational tool to achieve the isolation of (CTC) and achieve the highest efficiency of cell capture and separation.

Methods: The behavior of cells in blood fluid, (RBC), (WBC), (CTC), was characterized by analyzing the critical strain pressure. The design of the filtration device is carried out through a variation of the flow, geometry, critical streamline analysis and vortex generation, selecting the best hydrodynamic condition generated due to the favorable behavior of cell classification.

Results: A critical pressure for white cells of P_{cr} = 33*MPa* was obtained; for the cancer cells, a critical pressure of P_{cr} = 20.2*MPa* for a viscosity of μ = 100*Pa.s*, up to P_{cr} = 60.3*MPa* for a viscosity μ = 200*Pa.s*. At hematocrit Ht=2-4%, the microfilter device in the bifurcation separates cancer cells with diameters between (D=14-20μm) and viscosities between (μ=20-200Pa·s) with an efficiency of 99%.

Conclusions: The final geometry was evaluated and the efficiency of the device that performs the filtering process was determined. In the first stage, cancer cells are captured with 99% efficiency. The designed filter generates 99% purity by sorting CTCs without contamination from red blood cells or white blood cells.

Study limitations: Meshes with element size smaller than S=0.2μm were not implemented due to the computational cost.

Keywords: Microfilter, Cell Sorting, Droplet, (MEMS), (RBC), (CTC).

Resumen

Introducción: El artículo es producto de la investigación "Diseño y simulación de dispositivo de microfiltración para el aislamiento de células tumorales circulantes desarrollado en la Universidad Industrial de Santander en el año 2022"

Objetivo: Diseñar un dispositivo para clasificar y separar células tumorales circulantes en fluido sanguíneo mediante el uso de herramienta computacional de dinámica multifísica para lograr el aislamiento de (CTC) y lograr la mayor eficiencia de captura y separación celular.

Métodos: Se caracterizó el comportamiento de las células en fluido sanguíneo, (RBC), (WBC), (CTC), mediante el análisis de la presión crítica de deformación. El diseño del dispositivo de filtración se realiza mediante una variación del flujo, geometría, análisis de línea de corriente crítica y generación de vórtice, seleccionando la mejor condición hidrodinámica generada debido al comportamiento favorable de clasificación celular.

Resultados: Se obtuvo una presión crítica de la célula blanca de P_{cr} = 33*MPa*, para las células cancerígenas una presión critica P_{cr} = 20.2*MPa* para una viscosidad de μ = 100*Pa.s* hasta P_{cr} = 60.3*MPa*, para una viscosidad μ = 200*Pa.s*, en hematocrito Ht=2-4% el dispositivo microfiltro en la bifurcación separa las células cancerígenas con diámetros entre (D=14-20μm) y viscosidades entre (μ=20-200*Pa·s)* con eficiencia de 99%.

Conclusiones: Se evaluó la geometría final y se determinó la eficiencia del dispositivo que realiza el proceso de filtrado, en la primera etapa se capturan las células cancerígenas con un 99% de eficiencia. El filtro diseñado genera una pureza del 99% al clasificar los CTC sin contaminación de glóbulos rojos o glóbulos blancos.

Limitaciones de estudio: No se implementaron mallados con tamaño de elemento menores a S=0.2μm por el costo computacional.

Palabras clave: Microfiltro, Separación celular, Gotas, (MEMS), (RBC), (CTC).

Resumo

Introdução: O artigo é produto da pesquisa "Desenho e simulação de um dispositivo de microfiltração para o isolamento de células tumorais circulantes desenvolvido na Universidade Industrial de Santander no ano de 2022"

Objetivo: Projetar um dispositivo para classificar e separar células tumorais circulantes no fluido sanguíneo usando uma ferramenta computacional de dinâmica multifísica para obter o isolamento de (CTC) e obter a maior eficiência de captura e separação de células.

Métodos: O comportamento das células no fluido sanguíneo (RBC), (WBC), (CTC) foi caracterizado pela análise da pressão de deformação crítica. O dimensionamento do dispositivo de filtração é realizado por meio da variação do fluxo, geometria, análise da linha de corrente crítica e geração de vórtices, selecionando a melhor condição hidrodinâmica gerada devido ao comportamento favorável da triagem celular.

Resultados: Obteve-se uma pressão crítica de P_{cr} = 33*MPa* para os glóbulos brancos, para células cancerígenas uma pressão crítica de P_{cr} = 20.2*MPa* para uma viscosidade de μ = 100*Pa.s* até P_{cr} = 60.3*MPa*, para uma viscosidade de μ = 200*Pa.s*, em hematócrito Ht=2-4% o dispositivo de microfiltro na bifurcação separa células cancerígenas com diâmetros entre (D=14-20μm) e viscosidades entre (μ=20-200*Pa·s)* com 99% de eficiência.

Conclusões: A geometria final foi avaliada e determinada a eficiência do dispositivo que realiza o processo de filtragem.Na primeira etapa, as células cancerígenas são capturadas com 99% de eficiência. O filtro projetado gera 99% de pureza classificando os CTCs sem contaminação de glóbulos vermelhos ou glóbulos brancos.

Limitações do estudo: Malhas com tamanhos de elemento menores que S=0,2μm não foram implementadas devido ao custo computacional.

Palavras-chave: Microfiltro, Separação celular, Gotículas, (MEMS), (RBC), (CTC).

1. INTRODUCTION

The migration of circulating tumor cells (CTCs) in the bloodstream to other organisms occurs when the cancer cell detaches from the primary tumor, filters into the blood vessels (intravasation), and migrates in the bloodstream to other organisms in the body (extravasation). This process is one of the deadly characteristics of cancer also known as metastasis [1], [2], [3], [4], [5].

The computed tomography method [6] is a detection method that can determine the size of the tumor and determine its growth through follow-up images. The treatment takes months between each shot and it is not always possible to know if the tumor is proliferating or sleeping.

For the characterization of cancer cells and white and red blood cells, the mechanical properties of the cell membrane, diameter and the viscosity of each type are defined according to the literature table I. Then we subject the cell to deformation by measuring the critical pressure, which is then compared and validated with micropipette models and simulations of cells through microfilters.

With the established cell models, we design the filtration device by a variation of the flow and geometry, and the best hydrodynamic condition generated is selected. For the favorable behavior of cell classification, in the first stage, CTCs with a diameter between $D = 12 — 18\ \mu m$ are filtered, in the second output, white cells are captured with a diameter between $D = 14\ \mu m$ along with red blood cells (RBCs).

For the simulations, the mesh is generated in two dimensions using quadrilateral elements structured in a transient model and using the volume fraction VOF method with the COUPLED algorithm using the ANSYS FLUENT solver.

For the capture efficiency, the percentage of CTCs captured in the outlet is determined, established by their separation, concerning the total number evaluated. The purity percentage measures the purity of the captured sample, determined by the volume percentage of white cells and red cells that are not filtered.

Finally, the efficiency and purity data are compared with the designs available in the literature, the data is plotted and the model is validated, demonstrating superior capture efficiency by achieving a higher processing volume.

1.1. SIZE AND DEFORMABILITY OF CANCER CELLS

Cancer cells are larger compared to erythrocytes, but can be similar in size to white blood cells with variable sizes depending on the type of leukocyte (monocyte, granulocyte). In examinations of tissue samples, epithelial cells (solid tumor cells) are always larger than all blood cells including leukocytes based on primary tumor tissue biopsies [7].

Cancer cells can be variable and present a challenge in modeling them. One of the reasons is that the surface tension can be found in a range from 0.001 mNm^{-1} to 1000 times this value. Some cells behave as a liquid drop within the fluid, so they present a characteristic surface tension; the ''cortical tension'' or "the area expansion modulus" with unit of measure in ($pN/\mu m$). On the other hand, the deformations of the lipid membrane require much larger tensions, which can also be expressed in the following equivalent units ($1\ nN/\mu m = 1\ mN/m = 1\ dyne/cm$); the latter is the most common form when measuring the surface tension of cell membranes [8].

On the other hand, in the work developed by [9], they determined the critical pressure necessary to generate the passage of a CTC through a microfilter, in which viscosities of less than 1 $Pa{\cdot}s$ were conveniently selected. In order to validate the results with theoretical models of critical, viscous and superficial pressure, for the design purposes of this project, the data of viscosities greater than 10 $Pa{\cdot}s$ are selected

e-ISSN 2357-6014 / Vol. 19, no. 1 / january-april 2023 / Bogotá D.C., Colombia
Universidad Cooperativa de Colombia

for cancer cells, with viscosities greater than 10 *Pa·s*, being real data of the nature of the cancer cell.

The affectation of conditions such as the hematocrit level was evaluated in [10], along with: the channel size and flow velocity on the behavior of a CTC in blood fluid, the flow of red cells with hematocrit between Ht(0.1 — 0.3) in a straight channel with a length of L = 47 *μm* and channel diameters between D(10 — 20 *μm*). After evaluating the lateral migration of the CTC in the channel, it was determined that high levels of hematocrit (Ht>0.3) prevent adhesion cells of the CTC to the wall. For a lower hematocrit (Ht<0.1, Ht<0.2), the CTC adheres to the wall in a time of approximately (t=0.2s), concluding that for hematocrit levels lower than (Ht<0.1) the cell adhesion of the CTC is greater, with a rapid response of adhesion of the CTC to the walls as shown in Figure 1. In the investigation, two channels with diameter size D (15-20μm) were evaluated. For a lower hematocrit (Ht=0.1), the CTC adhesion response to the wall was faster in the channel with the largest diameter D=20μm according to the level of confinement, in which if the confinement of the CTC cell is $(D/D_T)<2$, where "D_T" is the diameter of the CTC and "D" is the diameter of the channel, if the confinement level is less than 2, the CTC can keep away from the wall and stay in the main flow, while for $(D/D_T)>2$ the CTC cell is displaced towards the walls [11].

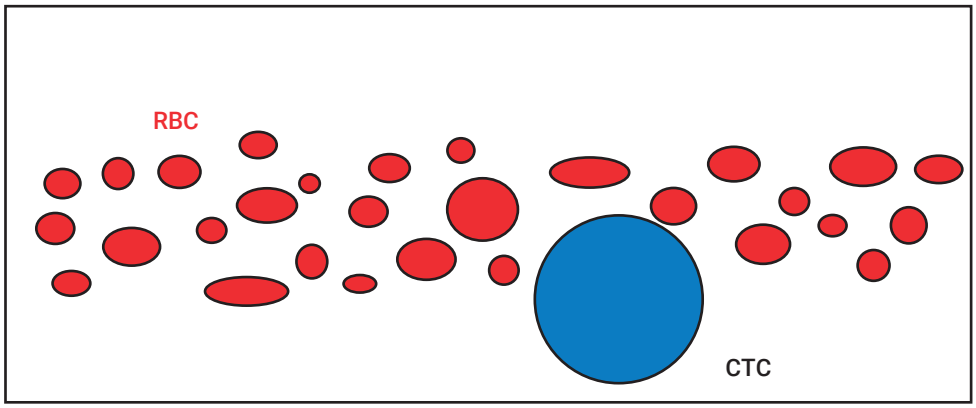

Figure 1. Migration of the blood cell CTC in a micro channel towards the walls.
Source: Own work

Another important factor is the relative resistance to flow; with the increase in the diameter of the channel, the relative resistance to flow is lower for CTC cells. In the simulations, they found that for a specific flow rate ($\gamma = 17.72s^{-1}$), the CTC detaches from the wall due to the increasing lifting force, but after a short time, the red blood cells flowing towards the center of the vessel expel the CTC from the red blood cell

center and further initiate adhesion of the CTC to the vessel wall, concluding that at high flow rates, for microchannel diameters greater than the diameter of the cancer cell and due to the effect of red blood cell aggregation in the center of the channel, cancer cells move towards the walls. It is finally concluded that with low levels of hematocrit (Ht<0.1), channel diameters much larger than the size of cancer cells (CTCs), and for high flow rates, they produce migration of the CTC towards the walls.

1.2. LEUKOCYTES (WHITE BLOOD CELLS).

Unlike erythrocytes (Red blood cells), leukocytes (White blood cells), WBC for its acronym, are part of the immune system. They protect the body from diseases or external agents and have the ability to travel to the tissues through the walls, by adhesion, to reach the infection.

Leukocytes are characterized by having different types of cells within this group. Initially, we have granulocytes with a diameter size between $D(10 - 20\mu m)$, lymphocytes with a size of $D(5.2 - 10.1\mu m)$, and monocytes with size between $D(10 - 20\mu m)$, $D(12 - 20\mu m)$, being the largest immune cell type within leukocytes.

Neutrophils are the most abundant types of granulocytes in the entire human body with a coverage between 40-70% of all white cells in the body with a size between D=12 — 15μm. The viscous difference between the inner nucleus and the viscosity of the cell cytoplasm, along with a low surface tension compared to red cells or cancer CTC cells, cause a non-Newtonian fluid behavior in the white cell. Due to their high viscosity, white cells are rigid, but they have a low surface tension, which gives them the ability to increase the surface area and deform (greater plasticity) to overcome smaller diameter blood vessels. The viscosity of blood cells is measured in (1 *poise* = $0.1 Pa{\cdot}s = dyn{\cdot}s/cm^2$) [12].

After subjecting neutrophils to a micropipette study with pressure differences from (ΔP = 98 — 882 *Pa*), using pipettes with a diameter of (D=8-10µm), a study [13] showed that the white cell cytoplasmic viscosity is dependent on the applied suction pressure, specifically dependent on the shear rate of the fluid. The study found that as the suction pressure increases, the average cytoplasmic viscosity decreases in an exponential decreasing, being initially a viscosity of (μ=500Pa.s) for a pressure of (P=98Pa) and average viscosity of (μ=55Pa.s) for a suction of (P=882Pa), these data indicate that the cytoplasm in the neutrophil is a non-Newtonian fluid. Finally, the study concludes that the mechanical behavior of the neutrophil can be approximated as a power-law fluid.

e-ISSN 2357-6014 / Vol. 19, no. 1 / january-april 2023 / Bogotá D.C., Colombia
Universidad Cooperativa de Colombia

Research [14] carried out on the radial distribution of white blood cells in microtubes, was aimed at measuring the radial distribution of white blood cells (WBC) in blood flow in a channel of length L=3.5cm and diameter (D=69μm). The exit position was evaluated for an interval of wall shear stress (τ=0.1-2.0 Pa). The results obtained concluded that for an increase in the flow, the wall shear stress leads to a displacement between (30-50%) of the cells towards the center of the channel, while the minimum distance of the cells to the wall at high and low shear stress becomes a cell free layer of approximately 5.8μm.

1.3. ERYTHROCYTES (RED CELLS)

Erythrocytes are cells without a nucleus inside and their function is to transport the hemoglobin protein for oxygen transport, made up of iron in its structure, (red blood cell) (RBC) for its acronym, red in color and biconcave discoid shape, are characterized by their high deformability and can move between capillaries with diameters smaller than (D<3μm). The red cell is differentiated by its characteristic of having a membrane with a high modulus of deformation, which defines it as almost incompressible, therefore, it has a higher surface tension, low viscosity that allows the red cell to maintain the mass surface area, and high plasticity due to low viscosity. Erythrocytes have an average diameter between (D=6-8.5μm) [15].

Fahraeus and Lindqvist [16] reported a change in blood composition (and consequent change in blood viscosity) when blood flows through a capillary tube with diameter less than D<0.3 mm, which is also known as the Fahraeus effect. They explain that the blood cells are transported in the fast axial flow while the plasma moves in a slow marginal current or cell free layer, see Figure 2. Then the average speed of the blood cells is greater than the plasma particles.

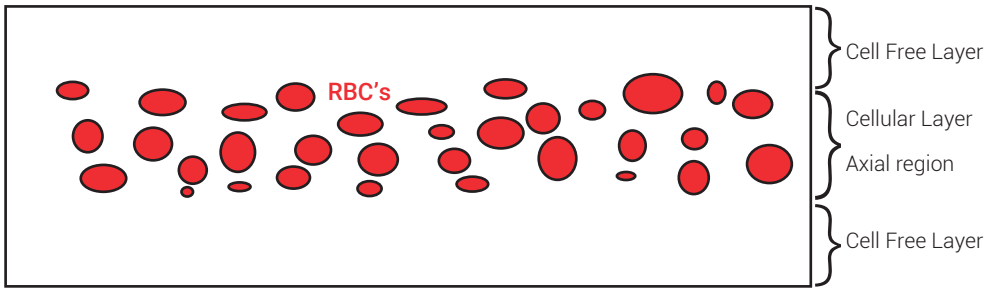

Figure 2. Aggregation of erythrocytes in straight channels and cell free layer
Source: Own work

e-ISSN 2357-6014 / Vol. 19, no. 1 / january-april 2023 / Bogotá D.C., Colombia
Universidad Cooperativa de Colombia

Cécile [17] found that lateral confinement or channel flow induces another phenomenon also associated with particle deformability: the migration of red blood cells away from the wall. The associated lift force is enough to make an isolated RBC go to the center in the D=30μm wide channel, see Figure 3. The strong lateral confinement in the D=30μm wide channel has a tremendous impact on the formation and stability of the structure; the fluid velocities were between $v(0.0008 - 0.004\ m/s)$ for a straight channel with a length of (L=6000μm).

For low hematocrit and a channel width of D=30μm, regular and stable bands are formed since the effect of the lateral wall is felt throughout the width of the channel. As shown in Figure 3, for hematocrit between (2 and 4%), a single band of centered red cells is formed; for hematocrit between (5% and 9%), more bands of blood cells begin to be generated in the channel, preserving a cell free layer of $Cfl = 10\mu m$.

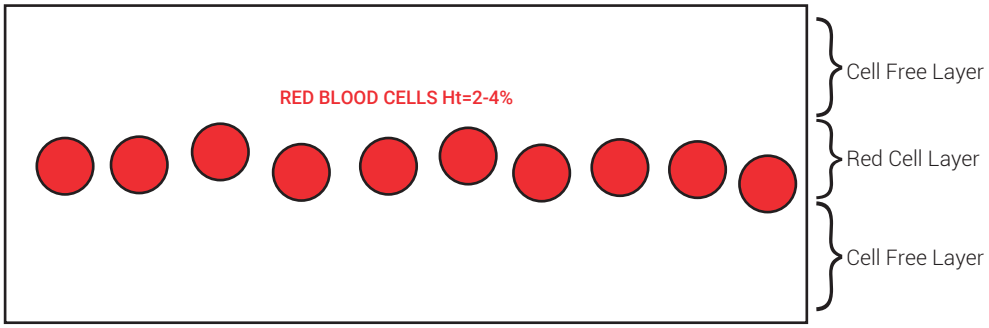

Figure 3. Self-organization of red blood cell suspensions under confined 2D flows
Source: Own work

Research [18] has been carried out for the development of a microfilter device for the separation of blood plasma from red cells, reaching high efficiency e>80% and high purity. During development, they determined the effect produced by the application of an obstruction in the width of the critical stream by placing it right in the place of the bifurcation for the capture of the plasma. Using two-dimensional simulations with ANSYS-Fluent software, it was determined that an obstruction with an inclination reduces the width of the critical current and the shape of the ramp promotes the formation of recirculation zones (vortices), which increases resistance to the passage of red blood cells through the lateral channels.

1.4. CELL CHARACTERIZATION THEORETICAL MODEL

For a blood sample flowing through a device, the total pressure applied to the device must overcome the two main components of the droplet: pressure due to the fluid

of the medium, and the pressure of the droplet due to the surface tension of the cell when they are in contact with the walls of the microfilter

$$\Delta P_{total} = \Delta P_{flow} + \Delta P_{surface\ tension} \quad (1)$$

The pressure drop due to the flow of the medium consists mainly of the pressure drop due to the viscosity of the droplet (ΔP_{hyd}) and pressure drop due to expansion and contraction in the microfilter.

$$\Delta P_{flow} = \Delta P_{hyd} + \Delta P_{contraction-expansion} \quad (2)$$

Viscous dissipation of fluid mechanical energy due to internal precision results in a pressure drop in the direction of flow. Pressure can then be calculated using the Hagen-Poiseuille equation which relates viscous pressure drop and flow rate. Where ΔP_{hyd} is the channel viscous pressure drop, R_{hyd} is the hydraulic resistance, and Q_v is the fluid volume flow, R_{hyd} is calculated using the equation developed by (Akbari et al). Knowing that the volume flow can be established as $Q_v = A \times v$, where A is the cross-sectional area and v is the linear velocity of the flow, we have. [19], [20], [21].

$$\Delta P_{hyd} = \frac{8\mu L v}{r^2} \quad (3)$$

Additionally, $\Delta P_{contraction\ -\ expansion}$ is caused by rapid contraction at the filter inlet and rapid expansion at the filter outlet, which can be calculated using the following relationship.

$$\Delta P_{contraction-expansion} = K_1 \frac{\rho U_1^2}{2} + K_2 \frac{\rho U_2^2}{2} \quad (4)$$

Where U_1 and U_2 are the flow velocities at the inlet and outlet of the filtration chamber, K_1 and K_2 are the constriction and expansion coefficients, respectively. These coefficients are set as 0.5 and 1 respectively. The viscous pressure is finally expressed as:

$$\Delta P_{flow} = \frac{8\mu L v}{r^2} + K_1 \frac{\rho U_1^2}{2} + K_2 \frac{\rho U_2^2}{2} \quad (5)$$

e-ISSN 2357-6014 / Vol. 19, no. 1 / january-april 2023 / Bogotá D.C., Colombia
Universidad Cooperativa de Colombia

The pressure generated by the surface tension ally, $\Delta P_{surface\ tension}$, can be determined using the Young-Laplace equation. If the flow in a microfilter is very low, the aspiration process of the cell in the filtration chamber can be approximated by a quasi-static process. Assuming that the aspirated part and the part not staked have circular shapes, then the surface pressure has the following expression.

$$\Delta P_{surface\ tension} = 2\sigma\left(\frac{1}{r_{ch}} - \frac{1}{r_{cell}}\right) \tag{6}$$

Where σ is the surface tension, ally, r_{ch} is the radius of the aspiration chamber and r_{cell} is the radius of the cell of the non-aspirated part during deformation [22].

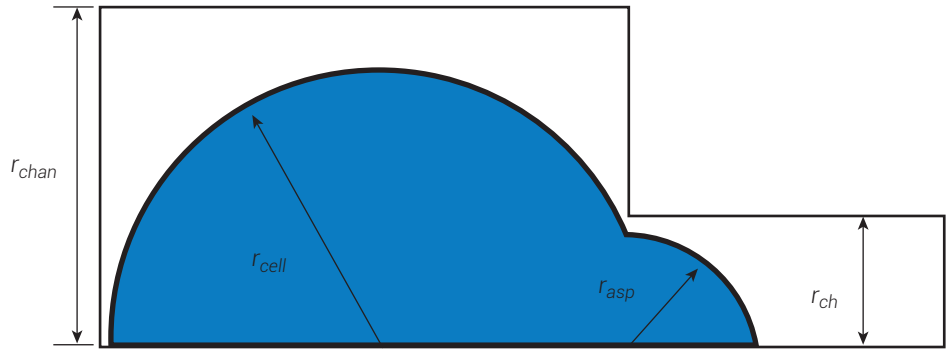

Figure 4. Cell squeezing through a filter
Source: Own work

1.5. COMPUTATIONAL MODELING (VOLUME OF FLUID METHOD ‘’VOF’’)

Incompressible fluids in motion are described by the Navier-Stokes equations that solve multiple fluid problems in behavior [23]. Any method for (CFD) of incomprehensible transient two-phase flows needs to solve the continuity and Navier-Stokes equations together with the interfacial jump conditions

$$\nabla . \mathbf{u} = 0 \tag{7}$$

$$\frac{\partial \rho u}{\partial t} + \nabla . \rho u \mathbf{u} = -\frac{\partial P}{\partial x} + \nabla . \left(\mu(\nabla u + \nabla^T u)\right) + F_s \tag{8}$$

e-ISSN 2357-6014 / Vol. 19, no. 1 / january-april 2023 / Bogotá D.C., Colombia
Universidad Cooperativa de Colombia

$$\frac{\partial \rho y}{\partial t} + \nabla . \rho y \mathbf{u} = -\frac{\partial P}{\partial y} + \nabla . \left(\mu(\nabla y + \nabla^T y)\right) + F_s \quad (9)$$

$$\frac{\partial \rho z}{\partial t} + \nabla . \rho z \mathbf{u} = -\frac{\partial P}{\partial z} + \nabla . \left(\mu(\nabla z + \nabla^T z)\right) + F_s \quad (10)$$

$$\frac{\partial F}{\partial t} + \mathbf{u} \cdot \nabla F = 0 \quad (11)$$

Equations 8-10 represent Newton's second law in which the rate of momentum is equal to the sum of forces on the fluid particle to represent the Navier-Stokes equation for a Newtonian fluid [24]. Equation 7 represents the conservative form of the transport equation for F. Where **u** is the flow velocity, P is the pressure shared by the two phases, and F is the volume fraction in a cell that is rated between 0 and 1. For a filled cell with the second phase, the phase is F=1, while for a filled cell with the primary phase F=0. For Equation 11, the motion of two immiscible interfaces of different densities and viscosity is described using a discrete function.

2. MATERIALS AND METHODS

2.1. CELL MODEL DESCRIPTION

The geometry of the filter is shown in Figure 5, with dimensions at the entrance (D_{inlet}) and an obstruction ($D_{chamber}$). The cell (CTC) is specified with the diameter (D_{cell}). For the characterization of cancer cells, the mechanical properties of the cell membrane and the viscosity (μ_{CTC}) for cancer cells are defined according to the literature, with a diameter of (D_{CTC}), and surface tension of (σ_{CTC}). For white cells, the mechanical properties of the cell membrane and the viscosity of each type of cell are defined; for neutrophils with a viscosity between (μ_{wTC}) diameter between (D_{cell}) and surface tension (σ_{WTC}), the mechanical behavior of the neutrophil can be approximated as a power-law fluid.

e-ISSN 2357-6014 / Vol. 19, no. 1 / january-april 2023 / Bogotá D.C., Colombia
Universidad Cooperativa de Colombia

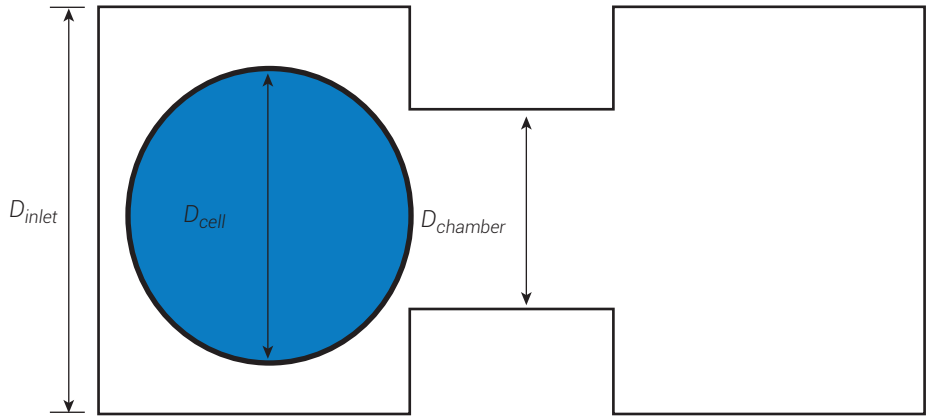

Figure 5. Microfilter device for cell characterization.
Source: Own work

In the strain-based microfilter, the white cell and the CTC are displaced through the filtration channel by the pressure imposed at the microfilter inlet called the system pressure, and its variation for time is called the pressure profile. System pressure is used to overcome resistance in the microfilter which is at maximum when the cell begins to enter the filtration channel. The maximum pressure of the system is generally called the critical pressure (P_{cr}).

2.2. MICROFILTER DESIGN

The geometry of the channels of the filtration device is defined taking into account the effect (Fahraeus-Lindqvist) is effective in channels of size between $S = 40\mu m - 300\mu m$ and the effects are pronounced for smaller size channels. As shown in Figure 6, in the first stage, the separation of cancer cells from erythrocytes and leukocytes is performed, and the definition of the geometry or domain is performed by defining a fluid input water as the discrete phase and oil as the continuous phase. Oil is supplied from the same source with an inlet flow rate (v_i). We use individual droplets to simulate cancer cells, white and red cells.

The channel with the (Droplets) has a width of (P_f) and a length of (l). This distance generates the effect of migration of the erythrocytes towards the center of the flow and the effect of diffusion that drives the more rigid bodies present in the blood such as the cancer cell (CTC) to move towards the wall of the channel [25], [26].

The red blood cells in the channel, simulated by taking a hematocrit Ht = 2% – 4%, accumulate in the center of the channel forming a single row or band of blood cells for small width channels for a channel width $A = 40 - 30\mu m$. The entrance of the

e-ISSN 2357-6014 / Vol. 19, no. 1 / january-april 2023 / Bogotá D.C., Colombia
Universidad Cooperativa de Colombia

cells in the microfilter bifurcation is simulated; according to previous estimations, the cancer cells in low hematocrit enter in a position close to the wall, while the red cells are positioned in a central band. The white cell is positioned within the group of red cells at a distance from the wall ($d = 6\mu m$), the minimum distance that a white cell can be found in straight channels.

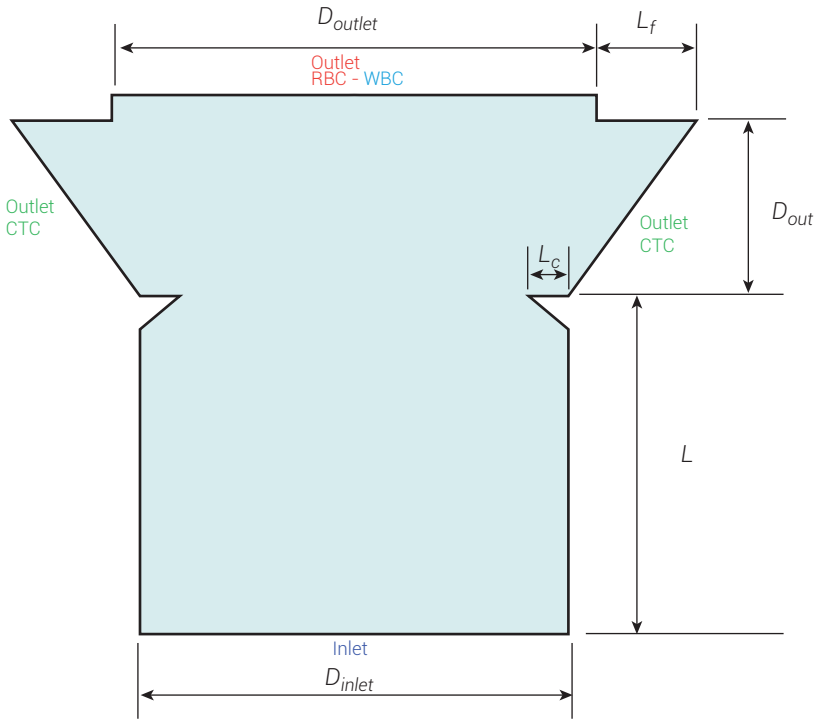

Figure 6. Microfilter device.
Source: Own work

The microfilter design proposal is based on applying the cell capture properties through the generation of vortices and analysis of fluid currents (critical stream analysis). A ramp-type constriction is used in the bifurcation, which allows us to generate vortices at the exit for the CTC. The generation of vortices in the lateral channel presents resistance to the passage of white and red cells, which are forced to remain within the main current by the action of drag. Cancer cells, on the other hand, the larger ones, collide with the obstruction. This effect causes the cell to move towards the lateral exit.

e-ISSN 2357-6014 / Vol. 19, no. 1 / january-april 2023 / Bogotá D.C., Colombia
Universidad Cooperativa de Colombia

Table 1. Model parameters

Parameter	Description	Value	Units	Ref.
D_f	Microfilter diameter	42	[μm]	
D_{out}	Outlet diameter	72	[μm]	
μ_{CTC}	CTC viscosity	20-200	[$Pa{\cdot}s$]	[27] [28] [29]
μ_{WBC}	WBC viscosity	130	[$Pa{\cdot}s$]	[30] [31]
μ_{RBC}	RBC viscosity	0,006	[$Pa{\cdot}s$]	[32] [33]
σ_{CTC}	CTC surface tension	0,05	[N/m]	[34] [35]
σ_{WBC}	WBC surface tension	0,000029	[N/m]	[36]
σ_{RBC}	RBC surface tension	0,005	[N/m]	[37]
D_c	Constriction diameter	30	[μm]	
L_c	Constriction length	4	[μm]	
D_{CTC}	CTC diameter	14-20	[μm]	[38] [39] [40]
D_{RBC}	RBC diameter	4-8	[μm]	[30] [35]
D_{WBC}	WBC diameter	12-14	[μm]	[34]
D_{cell}	Characterized cell diameter	16	[μm]	
V_i	Inlet velocity	0.03	m/s	

Source: Own work

3. RESULTS

In the first place, simulations are carried out to determine the critical pressure for viscosities between (μ = 0.01 – 0.04 *Pa.s*); for a superficial surface tension which is σ = 0.05*N/m*, the results are shown in Figure 7.

e-ISSN 2357-6014 / Vol. 19, no. 1 / january-april 2023 / Bogotá D.C., Colombia
Universidad Cooperativa de Colombia

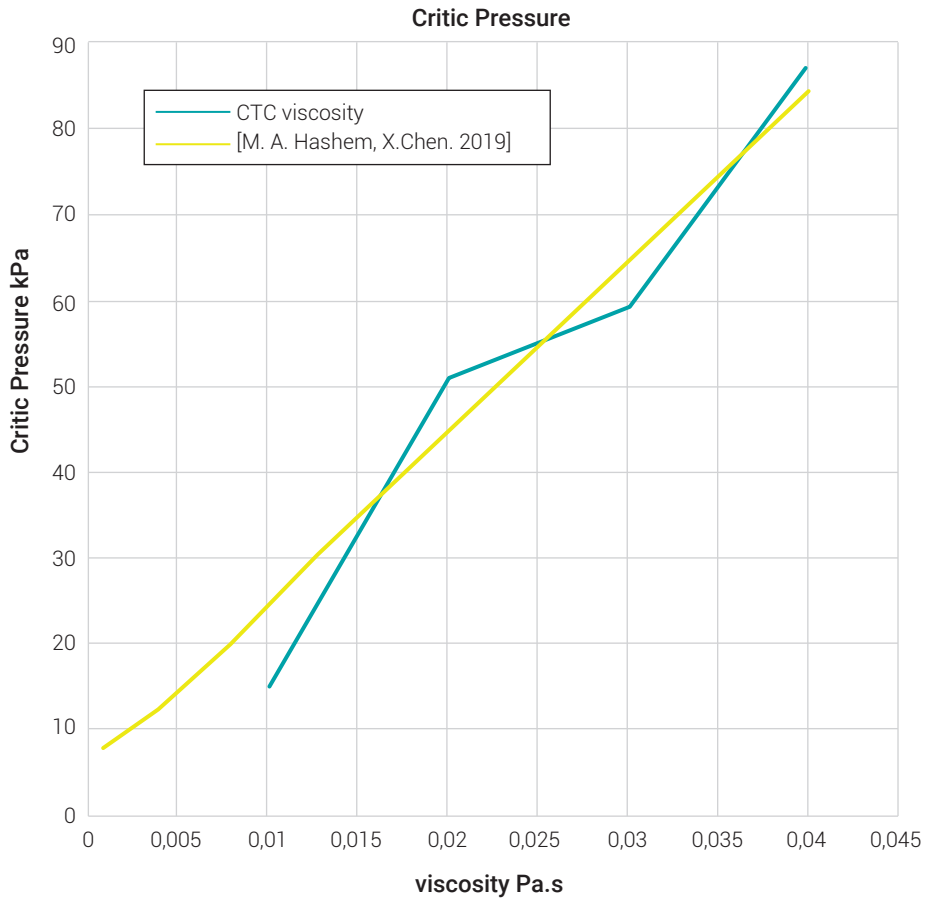

Figure 7. Results comparison.
Source: Own work

Figure 7, represents the comparison of data obtained for the set of cancer cells (CTC) with viscosities between (μ = 0.01 – 0.04 *Pa.s*)). The critical pressure results are compared with the results obtained by (M.A. Hashem, X. Chem. 2019): the error obtained for the viscosity cell (μ = 0.01 *Pa.s*) e = 39.2%, for the evaluated viscosity of (μ = 0.02 *Pa.s*) the error is e = 14.17%, while for the viscosity cell (μ = 0.03 *Pa.s*), the error is (e = 7.7%). Finally, for the CTC evaluated with a viscosity of (μ = 0.04 *Pa.s*), the error obtained is e = 3.53%, resulting in an average error percentage of $\bar{e}$ = 15.1%.

e-ISSN 2357-6014 / Vol. 19, no. 1 / january-april 2023 / Bogotá D.C., Colombia
Universidad Cooperativa de Colombia

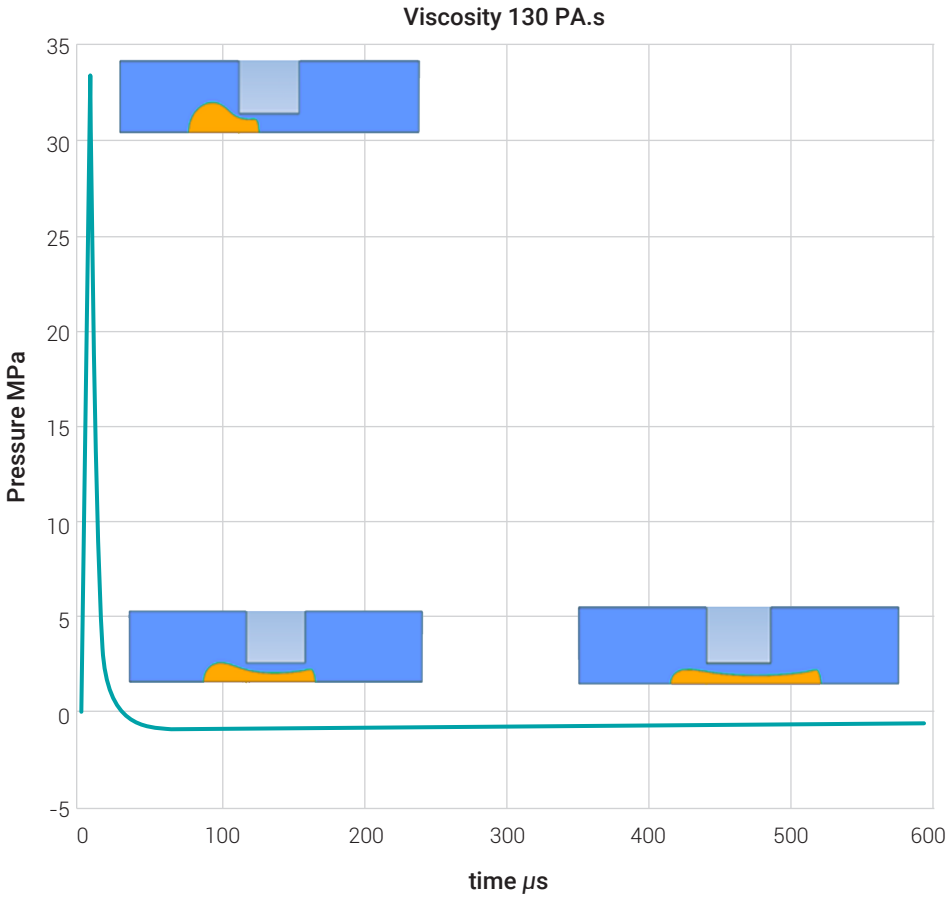

Figure 8. WBC Cell squeezing through a filter, viscosity $\mu = 130\ Pa.s$ (Power-law).
Source: Own work

Figure 8, represents the pressure profile on the neutrophil during the deformation process. The filtering stages in the graph show the non-Newtonian behavior. The critical pressure is quickly reached being $P_{cr} = 33MPa$. Then a rapid decrease in pressure is presented, due to the average viscosity of the cell being non-Newtonian and according to what is described in the literature. The rate of linear deformation increases during the filtration process. Finally, the cell behavior is governed by the equation (Power-law) that simulates the WBC as a non-Newtonian fluid.

e-ISSN 2357-6014 / Vol. 19, no. 1 / january-april 2023 / Bogotá D.C., Colombia
Universidad Cooperativa de Colombia

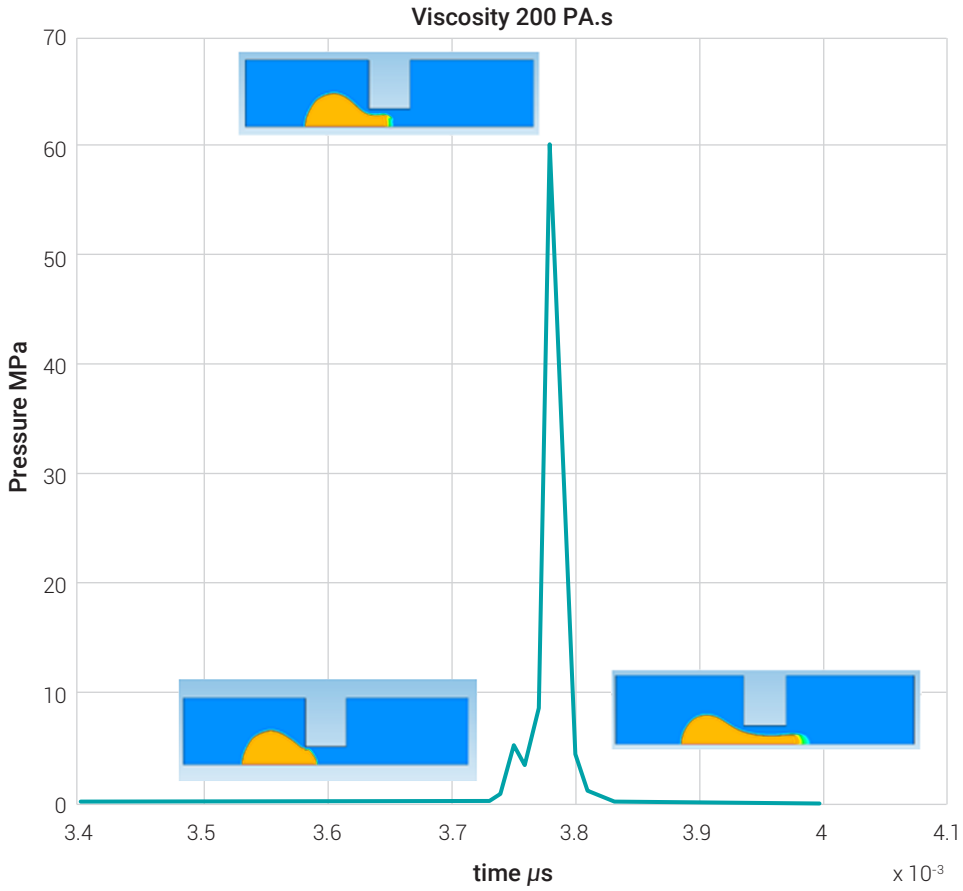

Figure 9. CTC Cell squeezing through a filter, viscosity 200 *Pa.s*.
Source: Own work

For the CTC with a viscosity of μ = 200 *Pa·s*, the maximum thrust presented is P_{cr} = 60.3 *MPa* according to the previous graph, with a greater time of deformation or displacement of the cell through the filter channel. This indicates that the pressure exerted is mainly viscous pressure given the high viscosity of the cell, to the extent that the viscosity increases the resistance presented by the surface tension, becoming negligible compared to the resistance produced due to cell viscosity.

e-ISSN 2357-6014 / Vol. 19, no. 1 / january-april 2023 / Bogotá D.C., Colombia
Universidad Cooperativa de Colombia

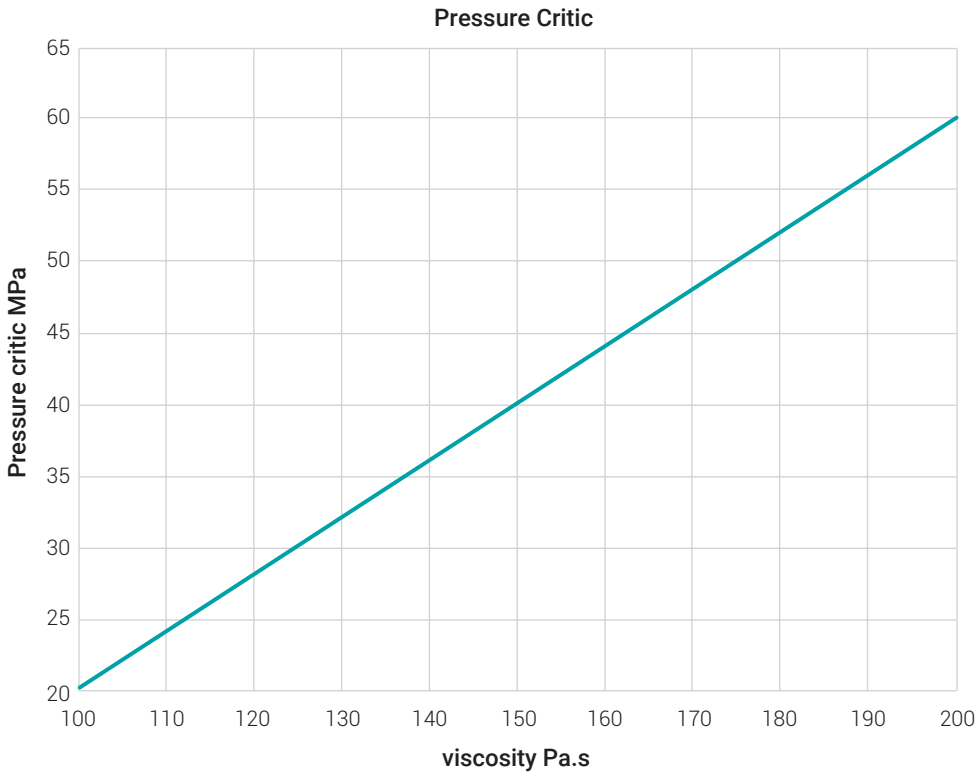

Figure 10. Critical pressure versus cell viscosity comparison.
Source: Own work

The critical pressure increases with the increase in viscosity. The increase in the critical pressure is proportional to the viscosity and is mainly dominated by the viscous pressure and not by the surface pressure, being from P_{cr} = 20.2*MPa* for a viscosity of μ = 100*Pa.s* up to P_{cr} = 60.3*MPa* for a viscosity of μ = 200*Pa.s*.

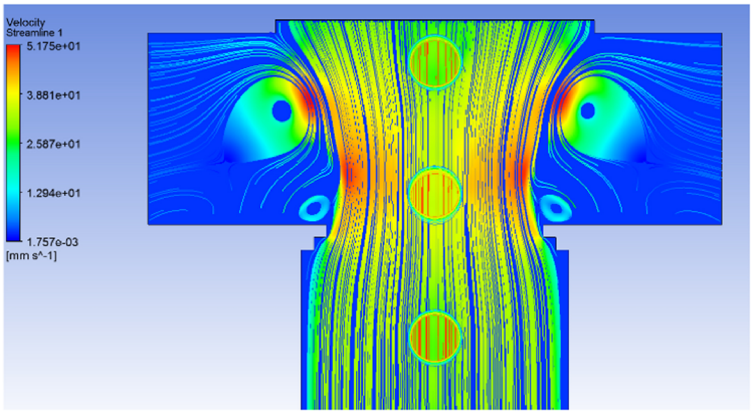

Figure 11. Formation of vortices and current with hematocrit *Ht* = 2 – 4%.
Source: Own work

e-ISSN 2357-6014 / Vol. 19, no. 1 / january-april 2023 / Bogotá D.C., Colombia
Universidad Cooperativa de Colombia

Blood flow simulation is performed with hematocrit between (Ht = 2 – 4%). Figure 11 represents the red cells passing through the bifurcation; red cells with a diameter of D=8μm are simulated, a band centered in the channel is simulated for the operation hematocrit.

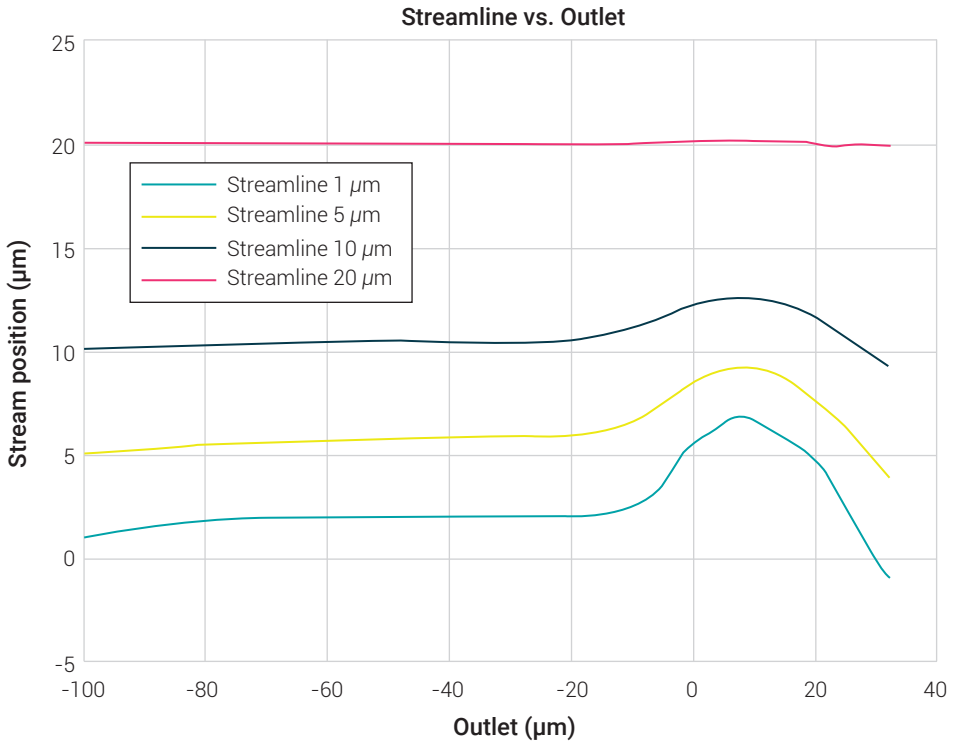

Figure 12. Variation of the position of the currents of the channel vs filter length.
Source: Own work

Figure 12, presents an analysis of the main fluid currents in different positions from the wall: x_1 = 1 *μm*, x_2 = 5 *μm*, x_3 = 10 *μm*, x_4 = 20 *μm*. The first position represents the closest distance to the channel wall, in which it shows that the current in the bifurcation presents a curvature towards the center of the channel. This deformation in the current is generated by the effect of the constriction, which projects the current towards the center of the channel. Followed in the bifurcation, the current maintains the curvature and is maintained in the main fluid, not moving towards the lateral outlet. This is due to the formation of vortices that maintain the current x_1, in the main channel, made evident as the currents x_2, x_3 tend to be positioned towards the center of the channel. The current stabilizes until reaching a straight direction in the main channel x_4.

e-ISSN 2357-6014 / Vol. 19, no. 1 / january-april 2023 / Bogotá D.C., Colombia
Universidad Cooperativa de Colombia

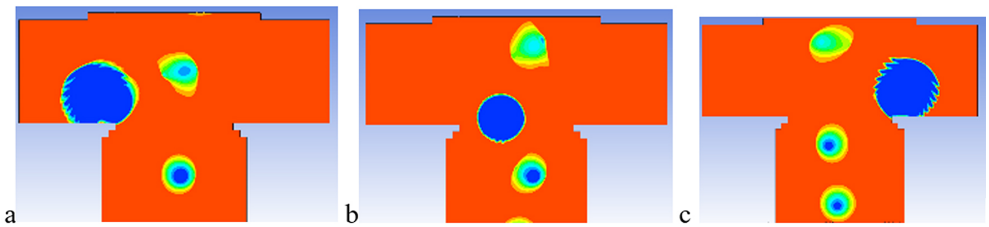

Figure 13. Cell exit positions a. CTC+RBCs, b. WBC+RBCs, c. CTC+RBCs.
Source: Own work

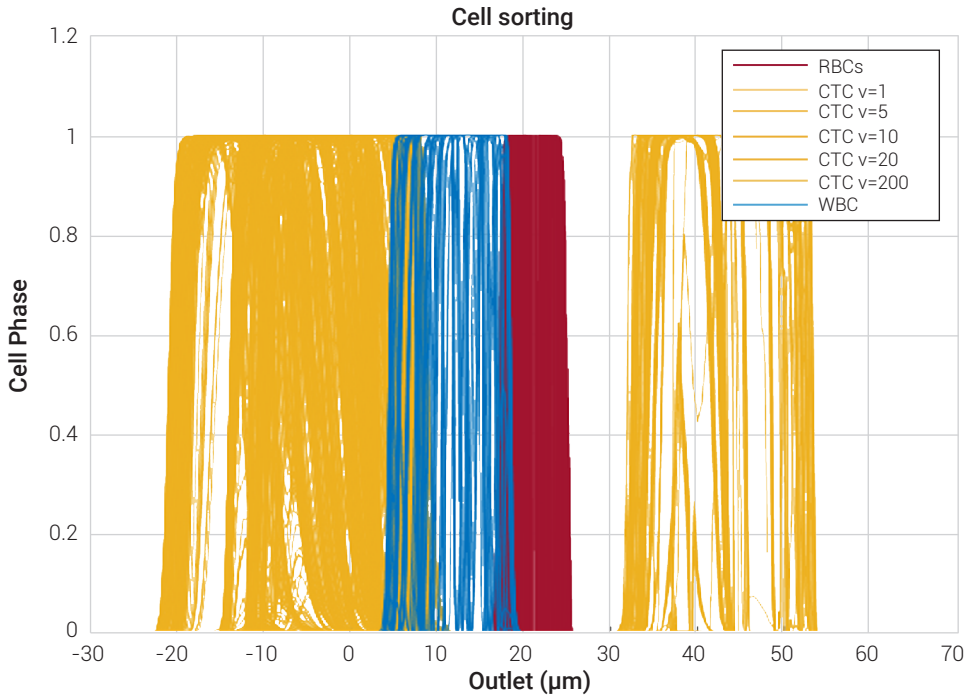

Figure 14. Classification of cells (CTC, WBC, RBC) in the microfilter.
Source: Own work

Figure 13 a-c and Figure 14, for the circulating tumor cell CTCs, the capture occurs at the bifurcation. Cells with viscosities between $\mu = 1 - 200 Pa.s$ were evaluated. The constriction obstructs their passage and deviates their direction towards the sides. The graph shows that all the CTCs evaluated near the wall are captured in the lateral outlet, which demonstrates the high capture efficiency of the device. The white cells are evaluated for the minimum distance with respect to the channel wall, being located at a distance of d=6µm, the minimum distance found in the literature. For said position in the flow, white blood cells manage to overcome the bifurcation, projecting towards the upper exit.

e-ISSN 2357-6014 / Vol. 19, no. 1 / january-april 2023 / Bogotá D.C., Colombia
Universidad Cooperativa de Colombia

Table 2. Particle isolation percentage.

Particle Isolation Percentage		
Microfilter	**Efficiency**	**Purification**
CTC microfilter	>90%	>90%
Vortex microfluidic technology [41]	75%	
spiral technology microfilter [42]	99.99%	

Source: Own work

In the first bifurcation phase, cancer cells with diameters between 14-20μm and viscosity between (20-200Pa·s) are captured with the efficiency of >90%. The vortex method maintains the purity of the separated sample by keeping the WBCs and RBCs in the mainstream, generating >90% sample purity, being white cells and red cells displaced towards the exit located at the end of the channel. The dissipative is compared with other designs, such as spiral technology for cell classification. The advantage of the designed microfilter is the ability to capture cells similar in size to a (WBC) but with greater rigidity, something that spiral technology does not achieve.

4. CONCLUSION

Cell characterization for the white cell shows its low resistance to deformation, and the ability to remain in the main current of the fluid, being affected by drag. The method (Power-law) reflects the real behavior of a white cell, which presents viscosities lower than the nominal viscosity of 130Pa.s and a high rate of deformation at high shear speeds. The cancer cells were taken as Newtonian because they had high viscosity and high rigidity. By increasing the viscosity, the critical pressure increased proportionally, reflecting that for higher the viscosities, the critical pressure is mainly due to the viscous pressure in the cell.

The designed microfilter device was carried out by studying the dynamic analysis of the fluid and the different types of blood cells (RBC, WBC) and circulating tumor cells (CTC). The analysis of the critical current determined the optimal flow rate and dimensions at the bifurcation channel diameter and size of constriction required to keep white and red cells within the main channel, whilst displacing CTC cells to the lateral outlet. In the bifurcation, the cancer cells evaluated with diameters between (14-20μm) and viscosities established between (20-200Pa s) are separated from the main fluid with an efficiency of 99.99%. The constriction takes advantage of the diffusion of the rigid cells and greater size, managing to differentiate cancer cells with a

e-ISSN 2357-6014 / Vol. 19, no. 1 / january-april 2023 / Bogotá D.C., Colombia
Universidad Cooperativa de Colombia

similar size to white cells but with greater rigidity, as well as CTC cells with a larger size, using constriction as an obstacle to generating the lateral displacement of the CTC.

5. ACKNOWLEDGEMENTS

This work is supported by the *Vicerrectoría de Investigación y Extensión (VIE)*. Code VIE -5373 of the *Universidad Industrial de Santander UIS,* where the research project has the grant to support Doctor's, Master's, and Bachelor's students in Mechanical Engineering, in the Robotics research area. Thanks to the DICBoT Research group for providing the facilities and laboratory tools.

6. REFERENCES

[1] T. Wu, and L. Fu, "Clinical Applications of Circulating Tumor Cells in Pharmacotherapy: Challenges and Perspectives," *Molecular pharmacology,* vol. 92, no. 3, pp. 232-239, 2017. doi:10.1124/mol.116.108142..

[2] P. Stanley, M. Leong, and W. William, "Micrometastatic cancer cells in lymph nodes, bone marrow, and blood: Clinical significance and biologic implications," *CA: a cancer journal for clinicians*, vol. 64, no. 3, pp. 195-206, 2014. doi:10.3322/caac.21217.

[3] M. Shyamala and A. H. Daniel, "Circulating tumor cells: a window into cancer biology and metastasis," *Current opinion in genetics & development*, vol. 20, no. 1, pp. 96-9, 2010. doi:10.1016/j.gde.2009.12.002.

[4] GeneticLab Co, L., "Circulating Tumor Cells". Circulating Tumor Cells. [Online]. Available: http://www.ctc-lab.info/english/ctc1/aboutc tc:html. (2021)..

[5] K. Molly, W. Yang and N. Sunitha, "The incorporation of microfluidics into circulating tumor cell isolation for clinical applications," *Current opinion in chemical engineering,* vol. 11, pp. 59-66, 2016. doi: 10.1016/j.coche.2016.01.005.

[6] S. P. Yadav, "Fusion of medical images in wavelet domain: an algorithmic model," *Revista Ingeniería Solidaria*, vol. 17, no. 1, pp. 1–23, Jan. 2021. https://doi.org/10.16925/2357-6014.2021.01.07.

[7] R. Harouaka, M. Nisic, S. Zheng, "Circulating tumor cell enrichment based on physical properties. Journal of laboratory automation," vol. 18, no. 6: 455-68, Jul. 2013. doi: 10.1177/2211068213494391.

[8] M. Aghaamoo, "Deformability-based circulating tumor cell separation with conical-shaped microfilters: Concept, optimization, and design criteria," *Biomicrofluidics*, vol. 9, no. 3, pp. 034106. Jun. 2015. doi:10.1063/1.4922081..

[9] M. Hashem, A. Mohammad, X. Chen, H. Tan, "An adaptive mesh refinement-based simulation for pressure-deformability analysis of a circulating tumor cell," *Proc. SPIE*, *Microfluidics, BioMEMS*, vol. XVII, pp. 108750L, March. 2019. doi: 10.1117/12.2507098

[10] L. Xiao, et al, "Effects of flowing RBCs on adhesion of a circulating tumor cell in microvessels. Biomechanics and modeling in mechanobiology," vol. 16, no. 2, pp. 597-610. Oct, 2016, doi:10.1007/s10237-016-0839-5.

[11] N. Takeishi, et al, "Flow of a circulating tumor cell and red blood cells in microvessels," *Physical Review*, vol, 92, no. 6, pp. 063011. 2015 doi: 10.1103/PhysRevE.92.063011

[12] J. K. Actor, "Cells and Organs of the Immune. Elsevier's Integrated Review Immunology and Microbiology," *Elsevier eBook on VitalSource*, 2nd Edition. 2012.

[13] R. M. Hochmuth, "Micropipette aspiration of living cells," *Journal of biomechanics,* vol. 33, no. 1 pp. 15-22. 2000. doi:10.1016/s0021-9290(99)00175-x.

[14] U. Nobis, A. R. Pries, G. R. Cokelet, P. Gaehtgens, "Radial distribution of white cells during blood flow in small tubes," *Microvascular research*, vol. 29, no. 3, pp. 295-304. May 1985. doi:10.1016/0026-2862(85)90020-2.

[15] D. Katanov, "Computer simulations of soft particles in flow," der Universität zu Köln. 2016.

[16] R. Fåhræus, T. Lindqvist, "The Viscosity of The Blood in Narrow Capillary Tubes," *American Journal of Physiology-Legacy Content*., vol. 96, no. 3, pp. 562–568, 1931 doi: 10.1152/ajplegacy.1931.96.3.562.

[17] I. Cécile, M. Dorian, M. Alexis, H. Delphine, C. Anne, M. Simon, V. et al., "Self-organization of red blood cell suspensions under confined 2D flows," *Soft Matter*, 2019. doi:10.1039/c8sm02571a.

[18] M. Sneha, B. Kumar, T. Chandra, A. Sen, "Development of a microfluidic device for cell concentration and blood cell-plasma separation," *Biomedical microdevices*, vol. 17, no. 6, pp. 115. December, 2015. doi:10.1007/s10544-015-0017-z.

[19] P. Sajeesh, M. Doble, A. K. Sen, "Hydrodynamic resistance and mobility of deformable objects in microfluidic channels," *Biomicrofluidics,* vol. 8, pp. 054112, 2014. https://doi.org/10.1063/1.4897332.

[20] M. Bahrami, M. Yovanovich, J. Culham, "A novel solution for pressure drop in singly connected microchannels of arbitrary cross-section," *Int. J. Heat Mass Transfer,* vol. 50, pp. 13–14, 2007. doi:10.1016/j.ijheatmasstransfer.2006.12.019

[21] M. Akbari, D. Sinton, M. Bahrami, "Viscous flow in variable cross-section microchannels of arbitrary shapes," vol. 54, no. 17-18, 2011 https://doi.org/10.1016/j.ijheatma sstransfer. 2011.04.028.

[22] M. Aghaamoo, Z. Zhang, X. Chen, and J. Xu, "Deformability-based circulating tumor cell separation with conical-shaped microfilters: Concept, optimization, and design criteria," *Biomicrofluidics,* vol. 9, no. 3, pp. 034106. Jun. 2015. doi:10.1063/1.4922081.

[23] A. Jafari, P. Zamankha, S.M. Mousavi, P. Kolari, "Numerical investigation of blood flow. Part II: In capillaries," *Communications in Nonlinear Science and Numerical Simulation*, vol. 14, no. 4, pp. 1396-1402, 2010. doi:10.1016/j.cnsns.2008.04.007.

[24] H. K. Versteeg, W. Malalasekera, "The finite volume method - An Introduction to Computational Fluid Dynamics -Second Edition". Pearson Education Limited 2007.

[25] M. Mehrabadi, N David. Ku, and K. Cyrus, "A continuum model for platelet transport in flowing blood based on direct numerical simulations of cellular blood flow," *Annals of biomedical engineering*, vol. 43, no. 6, pp. 1410-21, 2015. doi:10.1007/s10439-014-1168-4.

[26] L. L. Xiao, Y. Liu, and S. Chen, "Effects of flowing RBCs on adhesion of a circulating tumor cell in microvessels," *Biomechanics and modeling in mechanobiology,* vol. 16, no. 2, pp. 597-610, 2017. doi:10.1007/s10237-016-0839-5.

[27] X. Zhang, M. A. Hashem, X. Chen, and H. Tan, "On passing a non-Newtonian circulating tumor cell (CTC) through a deformation-based microfluidic chip," *Theoretical and Computational Fluid Dynamics*, vol. 32, no. 6, pp. 753–764, 2018. doi:10.1007/s00162-018-0.

[28] F. Y. Leong, Q. Li, C. Lim. K-H, "Modeling cell entry into a micro-channel," *Biomech Model Mechanobiol,* vol. 10, pp. 755–766, 2011. doi: https://doi.org/10.1007/s10237-010-0271-1.

[29] K. Wang, X. H. Sun, Y. Zhang, T. Zhang, Y. Zheng, Y. C. Wei, et al, "Characterization of cytoplasmic viscosity of hundreds of single tumour cells based on micropipette aspiration," *R. Soc. open sci.*, 6181707181707. 2019. doi: http://doi.org/10.1098/rsos.181707.

[30] R. Hochmuth, "Measuring the Mechanical Properties of Individual Human Blood Cells," *ASME. J Biomech Eng*, vol. 115, no. 4B, pp. 515–519. 1993. doi: https://doi.org/10. 1115/1.2895533.

[31] D. Cheng, Z. Nastaran, K. Konstantinos, "Biomechanics of the Circulating Tumor Cell Microenvironment," *Advances in Experimental Medicine and Biology. Biomechanics in Oncology*, vol. 1092, no. 11, pp. 209–233, 2018. doi:10.1007/978-3-319-95294-9_11

[32] F. Guglietta, M. Behr, L. Biferale, G. Falcucci, M. Sbragaglia, "On the effects of membrane viscosity on transient red blood cell dynamics," *Soft Matter*, vol. 16, pp. 6191-6205, 2020. doi:10.1039/D0SM00587H .

[33] T. Omori, T. Ishikawa, D. Barthes, A.-V. Salsac, Y. Imai, T. Yamaguchi, "Tension of red blood cell membrane in simple shear Flow," *PHYSICAL REVIEW E*., vol 86, pp. 056321, 2012. doi:10.1103/PhysRevE.86.056321 .

[34] Q. Guo, S. M. McFaul, H. Ma, "Deterministic microfluidic ratchet based on the deformation of individual cells," *Soft Matter,* vol. 83, pp. 051910, 2011. doi: 10.1103/PhysRevE. 83.051910.

[35] A. Preetha, N. Huilgol, R. Banerjee, "Interfacial properties as biophysical markers of cervical cancer," *Biomedecine & pharmacotherapie,* vol. 59, no. 9, pp. 491-7, 2005. doi:10.1016/j.biopha.2005.02.005.

[36] E. Evans, A. Yeung, "Apparent viscosity and cortical tension of blood granulocytes determined by micropipet aspiration," *Biophysical Journal*, vol. 56, no. 1, pp. 151–160, 1989. doi:10.1016/s0006-3495(89)82660-8..

[37] Y. C. Fung, "Biomechanics-Mechanical properties of living tissues-Second edition," Second ed. Springer. 1993. doi: https://doi.org/10.1007/978-1-4757-2257-4.

[38] F. Meyskens, S. Thomson, T. Moon, "Quantitation of the number of cells within tumor colonies in semisolid medium and their growth as oblate spheroids," *Cancer research,* vol. 44, no. 1, pp. 271-7, 1984.

[39] A. S. Kashani, M. Packirisamy, "Cellular deformation characterization of human breast cancer cells under hydrodynamic forces," *AIMS Biophysics*, vol. 4, no. 3, pp. 400-414, 2017. doi: 10.3934/biophy.2017.3.400.

[40] G. Thomas, M. Stamp, E. Melanie, W Achim, F. Thomas, "Hydrodynamic and label-free sorting of circulating tumor cells from whole blood," *Appl. Phys. Lett*., vol. 107, pp. 203702. 2015. doi: https://doi.org/10.1063/1.4935563.

[41] C. Renier, P. Corinne, C. Edward, L. James, E. Haiyan, C. Lemaire, et al, "Label-free isolation of prostate circulating tumor cells using Vortex microfluidic technology," *Precision Oncology*, vol. 1, no. 1, pp. 15, 2017. doi:10.1038/s41698-017-0015-0.

[42] D. González-Esparza, et al, "Design and Modeling of a Microfluidic Device with Potential Application for Isolation of Circulating Tumor Cells," *IEEE (ICEV)*, pp. 1-7, 2019. doi: 10.1109/ICEV .2019.8920484..